VIP Biocatalysis

DOI: 10.1002/anie.201209732

Resonance Raman Spectroscopy as a Tool to Monitor the Active Site of Hydrogenases**

Elisabeth Siebert, Marius Horch, Yvonne Rippers, Johannes Fritsch, Stefan Frielingsdorf, Oliver Lenz, Francisco Velazquez Escobar, Friedrich Siebert, Lars Paasche, Uwe Kuhlmann, Friedhelm Lendzian, Maria-Andrea Mroginski, Ingo Zebger,* and Peter Hildebrandt**

In memory of Gernot Renger

[NiFe] hydrogenases are key enzymes in the hydrogen metabolism in many microorganisms and oxidize molecular hydrogen reversibly at a heterobimetallic active site. The released electrons are usually transferred through three iron–sulfur clusters to the physiological redox partner.[1,2] The catalytic center has two metal ions Ni and Fe, which are bridged by two cysteinyl thiolates. Two further are bound to the Ni while the Fe is additionally coordinated by three diatomic ligands: one CO and two CN^-.[3] Different redox states of the bimetallic center are largely defined by the oxidation state of the Ni and the chemical nature of an additional ligand at a third bridging position between the two metals, which serves as the cleavage site for hydrogen.[4,5]

Elucidating fundamental processes of microbial energy conversion is essential to promote biotechnological applications of hydrogen as a clean fuel.[6] In this respect, a comprehensive understanding of the catalytic mechanism of hydrogenase requires the characterization of the active site structure of the species involved. Electron paramagnetic resonance (EPR) and infrared (IR) spectroscopy are well-established techniques for probing the various states of the catalytic cycle.[4,5] However, both methods are associated with inherent limitations. EPR spectroscopy is restricted to paramagnetic Ni states, whereas information about the active site Fe (Fe^{II}, $S = 0$) is largely inaccessible. IR spectroscopy probes all states of the active site by exploring the stretching vibrations of the diatomic ligands of the Fe. Thereby, it senses variations of the electron density distribution in the bimetallic complex, albeit without immediate insight into the structure of the [NiFe] center. In this respect, resonance Raman (RR) spectroscopy may be a powerful complementary technique as it allows the vibrational modes that involve the metal ions to be probed selectively, and thus, directly reflects the structural and electronic properties of the [NiFe] site.[7]

Herein we demonstrate, for the first time, the capability of RR spectroscopy to provide novel insights into the active site structure of a [NiFe] hydrogenase within a concerted experimental and theoretical approach. In view of the availability of crystal structure data and previous in-depth IR and EPR spectroscopic studies, we have chosen the oxygen-tolerant membrane-bound hydrogenase (MBH) from *Ralstonia eutropha* H16 (*Re*) as a model system.[8,9]

RR spectra of H_2-reduced MBH, measured with a 458 nm excitation at 79 K, display distinct vibrational bands between 400 and 650 cm^{-1} (Figure 1 A, black line), whereas comparable signals are not observed in the spectrum of the oxidized, as-isolated (untreated) enzyme. The monitored bands appear in the spectral range characteristic of Fe–CO/CN stretching and bending modes,[10] as also reported for hydrogenase model compounds.[11–13] Contributions from iron–sulfur cluster modes can be excluded as they are lower in frequency and, owing to the resonance enhancement through S→Fe charge-transfer transitions, primarily detectable in the oxidized states.[14] These conclusions are supported by Raman spectra calculated for the active site of the MBH by means of a hybrid quantum mechanical/molecular mechanical (QM/MM) model that was recently constructed on the basis of a computationally refined crystal structure of reduced MBH (for computational details, see the Supporting Information SI5).[2,15] In these calculations, RR intensities were approximated according to the contribution of Fe–CO coordinates to the potential energy distribution (PED) of individual modes to mimic the resonance enhancement by the metal–ligand charge-transfer transition. Indeed, spectra calculated for various states of the active site display distinct bands between 400 and 650 cm^{-1}, that is, in the range of the experimental RR bands (see Figure 1). Both the vibrational assignment and the assumption that an Fe→CO charge-transfer electronic transition is the origin for the resonance enhancement of these bands is confirmed by the RR spectrum of ^{13}C-labeled H_2-reduced MBH (Figure 1 A, red line), which displays distinct isotopic shifts for all major bands, as predicted by the QM/MM calculations (Figure 1 B–D, red lines). Only small isotopic shifts, on the order of 1 cm^{-1}, are observed upon

[*] E. Siebert,[+] M. Horch,[+] Y. Rippers,[+] F. Velazquez Escobar, Prof. Dr. F. Siebert, L. Paasche, Dr. U. Kuhlmann, Dr. F. Lendzian, Prof. Dr. M. A. Mroginski, Dr. I. Zebger, Prof. Dr. P. Hildebrandt
Technische Universität Berlin, Institut für Chemie, Sekr. PC14
Strasse des 17. Juni 135, 10623 Berlin (Germany)
E-mail: marius.horch@gmx.de
ingo.zebger@tu-berlin.de
hildebrandt@chem.tu-berlin.de
Dr. J. Fritsch, Dr. S. Frielingsdorf, Prof. Dr. O. Lenz
Institut für Biologie/Mikrobiologie, Humboldt Universität zu Berlin
Chausseestrasse 117, 10115 Berlin (Germany)
[+] These authors contributed equally to this work.

[**] Financial support by the DFG (Cluster of Excellence "UniCat"), Senat Berlin ("Nachhaltige Chemie").
Supporting information for this article is available on the WWW under http://dx.doi.org/10.1002/anie.201209732.

© 2013 Wiley-VCH Verlag GmbH & Co. KGaA, Weinheim

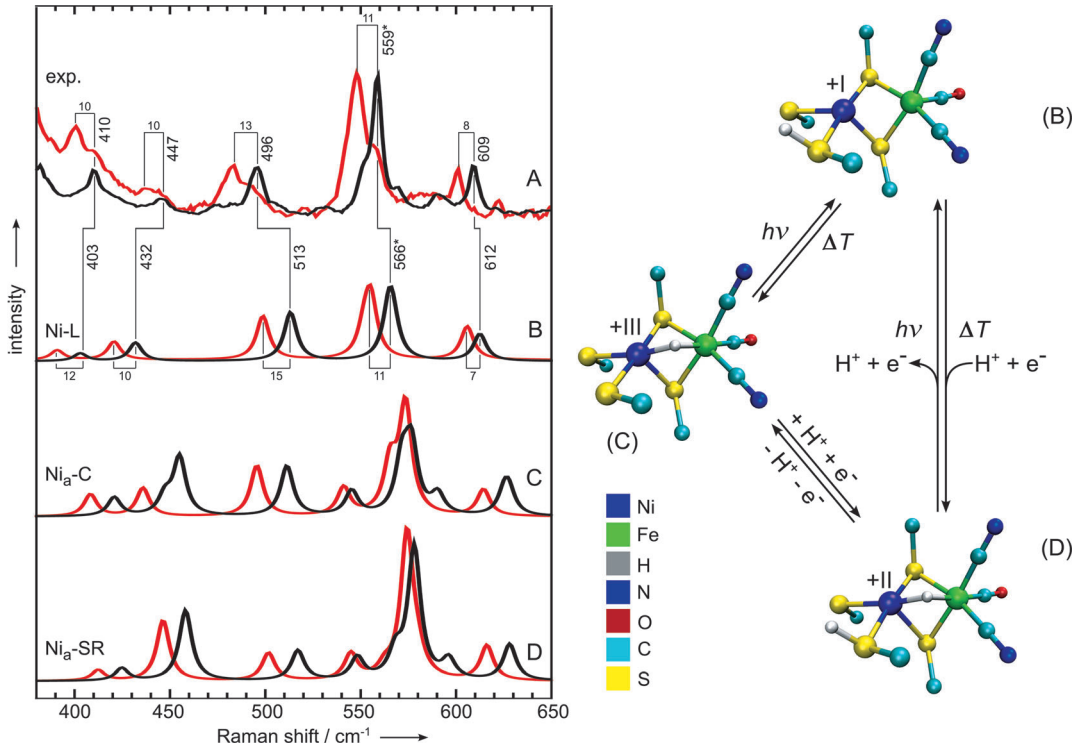

Figure 1. Left panel: A) Experimental RR spectra of H_2-reduced MBH, obtained with a 458 nm excitation, and calculated Raman spectra of the [NiFe] active site for B) Ni-L, C) Ni_a-C, and D) Ni_a-SR. Black trace non-labeled species; red trace ^{13}C-labeled species. Bands marked with an asterisk are related to the superposition of two closely adjacent normal modes (see Table 1) and, thus, the corresponding isotopic shifts are deduced from the apparent band maxima. Right panel: active site structure models of B) Ni-L, C) Ni_a-C, and D) Ni_a-SR.

^{15}N labeling, which is in line with the calculations (see Table 1). Based on these findings, the bands observed in the RR spectrum can be evidentially assigned to bending and stretching modes of the {Fe(CO)(CN$^-$)$_2$} moiety as also proposed in a recent nuclear resonance vibrational spectroscopy (NRVS) study.[16]

Like most other hydrogenases, H_2-reduced MBH has a mixture of catalytically active redox species as detected by IR spectroscopy:[17] Ni_a-C is the paramagnetic (Ni^{III}, $S = 1/2$) key intermediate in hydrogen cycling of [NiFe] hydrogenases, carrying a hydride ligand at the third bridging site between the two metals.[18] In contrast, the fully reduced Ni_a-SR state,

Table 1: Experimental frequencies and isotopic shifts of the active site modes of H_2-reduced MBH and calculated values for Ni-L, Ni_a-C, and Ni_a-SR (in cm^{-1}).[a]

Normal mode description[b] (Ni-L)	Experiment			Ni-L			Calculated Ni$_a$-C			Ni$_a$-SR		
	^{12}C, ^{14}N	Δ^{13}C	Δ^{15}N	^{12}C, ^{14}N	Δ^{13}C	Δ^{15}N	^{12}C, ^{14}N	Δ^{13}C	Δ^{15}N	^{12}C, ^{14}N	Δ^{13}C	Δ^{15}N
δ(Fe-C-O/N)	410	−10	−1	403	−12	−2	421	−12	−2	425	−12	−2
δ(Fe-C-N$_{Arg}$) ν(Fe-CN$_{Arg}$)	447	−10	−1	432	−11	−3	447 455	−12 –	−4 –	458	−12	−2
δ(Fe-C-N$_{Thr}$) ν(Fe-CO)	496	−13	−1	513	−14	−1	511	−16	−2	517	−15	−2
	552	−10	n.a.[c]	–	–	–	545	−4	−1	548	−3	−1
δ(Fe-C-O) ν(Fe-CO)	559	−11	−1	565 567	−10 −15	−1 −1	572 577	−6 −3	−1 −1	568 578	−5 −4	0 −1
	568	n.a.[c]	0	–	–	–	590	−16	0	596	−16	0
ν(Fe-CO)	609	−8	0	612	−7	−1	625 628	– −13	– −1	628	−12	0

© 2013 Wiley-VCH Verlag GmbH & Co. KGaA, Weinheim

which most likely carries the hydride ligand as well,[4] is EPR-silent (Ni^{II}, $S=0$). This species consists of up to three sub-states, which presumably differ in their protonation and spin state or their interaction with the protein environment.[4,5]

In principle, both Ni_a-C and Ni_a-SR may contribute to the RR spectrum. At low temperatures, however, irradiation of Ni_a-C with visible light, such as the Raman probe beam at 458 nm, may cause dissociation of the bridging hydride,[18] thereby forming the so-called Ni-L state (Ni^{I}, $S=1/2$), another potentially active intermediate, which also includes up to three sub-states.[18] To mimic the conditions of the RR experiments, we have recorded low-temperature IR and EPR spectra in the dark and under constant irradiation at 460 and 455 nm, respectively. The observed signals in the "light-minus-dark" difference spectra (Figure 2) can be assigned on the basis of previous studies:[17,19] CO/CN stretching vibrations and g-tensor components displayed in gray, represent the fraction of the enzyme in the Ni-L state formed at the expense of the Ni_a-C state (black), as indicated by the inverse sign of the spectroscopic features. These findings show an essentially complete Ni_a-C→Ni-L conversion, thereby excluding a contribution of the Ni_a-C state to the RR spectrum shown in Figure 1 A.

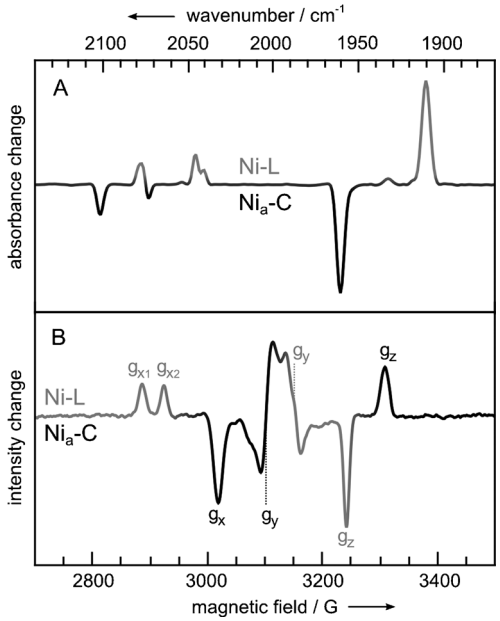

Figure 2. Light-induced low temperature difference spectra "light-minus-dark" of H_2-reduced MBH, obtained by A) IR and B) EPR spectroscopy. The black signals refer to Ni_a-C and light gray signals refer to Ni-L.

The spectroscopic experiments on the MBH were further extended to different reducing conditions (see Supporting information). IR spectroscopy indicates that the contribution of Ni_a-C strongly increases at the expense of Ni_a-SR, if the fraction of H_2 in the gas mixture is decreased from 100 to 5%, reflecting the higher reduction potential of Ni_a-C.[17] However, RR spectra recorded under both conditions were found to be identical in terms of band frequencies and intensities (see Figure SI6), indicating that equal amounts of the same redox state are probed under both conditions. This situation suggests that equilibria between all the reduced states are altered in favor of the detected species during the RR experiment, which is best explained by an efficient photoconversion into the Ni-L state caused by the Raman probe beam. Indeed, the RR signals vanish if the temperature is raised above 200 K, in line with the previously reported thermal decay of Ni-L.[4] Thus, we conclude that the RR spectra of H_2-reduced MBH solely reflect the Ni-L state whereas the resonance enhancement of the Ni_a-C and Ni_a-SR species is too weak to give rise to detectable RR signals at 458 nm.

Further support for this assignment is derived from the comparison with Raman spectra calculated for different redox, spin, and protonation states of the active site. The calculated spectra of most of these species differ substantially from the experimental spectrum and, thus, a more detailed inspection is restricted to the calculated spectra of the Ni_a-C, Ni-L, and Ni_a-SR states. For the Ni-L and Ni_a-SR states protonation at the Cys597 sulfur is assumed (Figure 1 B–D). Consistent with the calculations for all three species (see Supporting Information), the strongest band in the experimental spectrum (559 cm^{-1}) reflects two closely spaced modes of predominant Fe–CO bending and stretching character. However, only calculations for Ni-L reproduce both the experimental frequency and the ^{13}C isotopic shift ($\Delta\nu$) very well, whereas the calculations for Ni_a-C and Ni_a-SR over- and underestimate the frequency and the isotopic shift, respectively. Also the prominent Fe–CO stretching mode, observed at 609 cm^{-1} ($\Delta\nu=-8$ cm^{-1}) in the experimental spectrum, is in good agreement with that calculated for Ni-L (612 cm^{-1}, $\Delta\nu=-7$ cm^{-1}), in contrast to the distinctly overestimated values for Ni_a-C and Ni_a-SR. The calculated spectra of Ni-L also provide the best agreement for the Fe–CN bending (and stretching) modes in the RR spectrum below 550 cm^{-1}. Thus, the comparison with the calculated spectra confirms that RR spectroscopy exclusively probes the Ni-L state under the experimental conditions employed. Note that the good agreement with the spectrum calculated for Ni-L only refers to the species with a protonated Cys597 (see Supporting Information), thereby giving the first experimental indication of the previously proposed protonation of a terminal cysteine ligand in the active site of [NiFe] hydrogenases.[20]

According to the above observations, the amount of Ni-L probed by RR spectroscopy is independent of the initial Ni_a-C/Ni_a-SR ratio. Since Ni_a-C is in equilibrium with Ni_a-SR, photoconversion of Ni_a-C could cause a depletion of the Ni_a-SR state if the thermal Ni_a-SR→Ni_a-C redox transition took place at 79 K. However, this transition can be excluded since the "light-minus-dark" IR difference spectrum in Figure 2 does not display any negative signals arising from Ni_a-SR. Moreover, this thermal reaction would result in an overall increase in paramagnetic species upon irradiation, which is not observed in the corresponding EPR difference spectrum (see Figure 2). Thus, we conclude that there is a yet unknown

 © 2013 Wiley-VCH Verlag GmbH & Co. KGaA, Weinheim

direct photochemical reaction from Ni_a-SR to Ni-L that becomes an efficient reaction channel only under high photon flux, for example during the RR experiments.

In conclusion, we have presented the first RR spectroscopic characterization of the active site of a [NiFe] hydrogenase, thereby introducing a novel technique that might also be applied to the characterization of [Fe] and [FeFe] hydrogenases. Herein, RR spectroscopy was shown to provide valuable structural and mechanistic insights by directly probing Fe–CO/CN vibrational modes which reflect bonding properties of the catalytic center that are considered to be key parameters in the hydrogen cycling of hydrogenases.[21] Although these Fe–ligand modes are also detectable in NRVS experiments,[16] this experimentally more demanding technique suffers from a significantly lower spectral resolution that prevents an identification of specific states of the active site. Conversely, RR spectroscopy allows for an unambiguous redox-state assignment and, thus, a specific characterization of individual species. In concert with complementary spectroscopic and advanced theoretical methods, this technique also provides valuable information on subtle but important details of the active site. This includes first experimental indications for the presence of a protonated terminal cysteine residue at the active site in the Ni-L state and the possibility of a direct photoconversion of Ni_a-SR into Ni-L. Thus, this integrated approach is capable of elucidating structural and electronic details beyond the level of crystallographic data.[15]

Received: December 5, 2012
Revised: January 22, 2013

Keywords: [NiFe] hydrogenase · biocatalysis · EPR spectroscopy · IR spectroscopy · resonance Raman spectroscopy

[1] A. Volbeda, M. H. Charon, C. Piras, E. C. Hatchikian, M. Frey, J. C. Fontecilla-Camps, *Nature* **1995**, *373*, 580 – 587.
[2] J. Fritsch, P. Scheerer, S. Frielingsdorf, S. Kroschinsky, B. Friedrich, O. Lenz, C. M. T. Spahn, *Nature* **2011**, *479*, 249 – 252.
[3] R. P. Happe, W. Roseboom, A. J. Pierik, S. P. Albracht, K. A. Bagley, *Nature* **1997**, *385*, 126.
[4] W. Lubitz, E. Reijerse, G. M. van Gastel, *Chem. Rev.* **2007**, *107*, 4331 – 4365.
[5] A. L. de Lacey, V. M. Fernandez, M. Rousset, R. Cammack, *Chem. Rev.* **2007**, *107*, 4304 – 4330.
[6] R. Mertens, A. Liese, *Curr. Opin. Biotechnol.* **2004**, *15*, 343 – 348.
[7] T. G. Spiro, R. S. Czernuszewicz, *Methods Enzymol.* **1995**, *246*, 416 – 460.
[8] T. Goris, A. F. Wait, M. Saggu, J. Fritsch, N. Heidary, M. Stein, I. Zebger, F. Lendzian, F. A. Armstrong, B. Friedrich, O. Lenz, *Nat. Chem. Biol.* **2011**, *7*, 310 – 318.
[9] K. A. Vincent, J. A. Cracknell, O. Lenz, I. Zebger, B. Friedrich, F. A. Armstrong, *Proc. Natl. Acad. Sci. USA* **2005**, *102*, 16951 – 16954.
[10] K. Nakamoto, *Infrared and Raman Spectra of Inorganic and Coordination Compounds—Applications in Coordination, Organometallic, and Bioinorganic Chemistry*, 6th ed., Wiley, Hoboken, **2009**.
[11] H. S. Shafaat, K. Weber, T. Petrenko, F. Neese, W. Lubitz, *Inorg. Chem.* **2012**, *51*, 11787 – 11797.
[12] M. G. Galinato, C. M. Whaley, N. Lehnert, *Inorg. Chem.* **2010**, *49*, 3201 – 3215.
[13] C. J. Stromberg, C. L. Kohnhorst, G. A. Van Meter, E. A. Rakowski, B. C. Caplins, T. A. Gutowski, J. L. Mehalko, E. J. Heilweil, *Vib. Spectrosc.* **2011**, *56*, 219 – 227.
[14] T. G. Spiro, R. S. Czernuszewicz, S. Han in *Biological Applications of Raman Spectroscopy, Vol. 3*, (Ed.: T. G. Spiro), Wiley, New York, **1988**, pp. 523 – 553.
[15] Y. Rippers, M. Horch, P. Hildebrandt, I. Zebger, M. A. Mroginski, *ChemPhysChem* **2012**, *13*, 3852 – 3856.
[16] S. Kamali, H. Wang, D. Mitra, H. Ogata, W. Lubitz, B. C. Manor, T. B. Rauchfuss, D. Byrne, V. Bonnefoy, F. E. Jenney, M. W. W. Adams, Y. Yoda, E. Alp, J. Zhao, S. P. Cramer, *Angew. Chem.* **2013**, *125*, 752 – 756; *Angew. Chem. Int. Ed.* **2013**, *52*, 724 – 728.
[17] M. Saggu, I. Zebger, M. Ludwig, O. Lenz, B. Friedrich, P. Hildebrandt, F. Lendzian, *J. Biol. Chem.* **2009**, *284*, 16264 – 16276.
[18] M. Brecht, G. M. van, T. Buhrke, B. Friedrich, W. Lubitz, *J. Am. Chem. Soc.* **2003**, *125*, 13075 – 13083.
[19] M. E. Pandelia, P. Infossi, M. Stein, M. T. Giudici-Orticoni, W. Lubitz, *Chem. Commun.* **2012**, *48*, 823 – 825.
[20] C. Fichtner, M. van Gastel, W. Lubitz, *Phys. Chem. Chem. Phys.* **2003**, *5*, 5507 – 5513.
[21] G. J. Kubas, *Chem. Rev.* **2007**, *107*, 4152 – 4205.

 © 2013 Wiley-VCH Verlag GmbH & Co. KGaA, Weinheim